Published in a special symposium book on

Functional Fillers and Nanoscale Minerals

Edited by Jon J. Kellar
Published by

Society for Mining, Metallurgy, and Exploration, Inc.

Pages: 253-265

Synthesis of Silicon Carbide by Reaction Milling in a Dual-drive Planetary Mill

Debasis Chaira, B. K. Mishra, S. Sangal
Indian Institute of Technology Kanpur
INDIA

ABSTRACT

Reaction milling has become a very effective means of synthesizing compounds from the corresponding elemental constituents. In this of silicon carbide is synthesized from elemental silicon and graphite powder by high-energy reaction milling in a specially built dual drive planetary mill. Reaction milling in this type of mill is most affected by the size of the grinding media. The phase evolutions, particle size distribution and morphology of particles during milling are studied during a 40 hours grinding period. Particle size distribution shows considerable amount of material is below 10 micron. X-ray diffraction study indicates complete conversion of silicon and graphite to silicon carbide. The crystallite size varies from 10 micron from the start to 100 nm after 40 hours of milling. The SEM picture clearly reveals the progress of size reduction and the extent of agglomeration of particles.

1. INTRODUCTION

Silicon carbide is a promising filler material due to its good thermal and chemical stability. This is valid both during synthesis and under severe service conditions. The SiC particulates can be used with aluminium for synthesis of Al-SiC metal matrix composites. Aluminium based metal matrix composites are becoming very popular due to its lightweight, high strength to weight ratio, stiffness and wear resistance properties. The specific applications of these composites include engine blocks, pistons, brake-system components, seals, solid lubricants, wear and abrasion resistant structures, electromechanical contacts and chassis components. Owing to its high temperature electrical properties, high breakdown voltage, and high electron mobility silicon carbide is used in electronic devices that are particularly suitable for high temperature applications. It is also used in various other types of high temperature applications such as heating elements and refractory material for furnaces due to its high fracture strength, excellent wear and creep resistance, high resistance to corrosion, good thermal conductivity and relatively low coefficient of thermal expansion.

Silicon carbide can be produced by many methods (Vogt, et al., 1985; Canon et al., 1982). The traditionally method which is to a large extent is commercialized is known as the Acheson process. Here a solid-state reaction between sand and petroleum cokes at very high temperature (2500°C) in an electric arc furnace using two large graphite electrodes leads to the formation of silicon carbide. The commercial product has a large grain size and is invariably contaminated with oxygen. There is other several fabrication processes for obtaining SiC that include polymer pyrolysis, chemical vapor deposition (CVD) and even hot pressing. Liquid phase reactions have also been used to synthesize silicon carbide, as reported by Ritter (1995). Most of the above mentioned approaches require temperature higher than 1500°C. However, silicon carbide can also

be synthesized without heating, such as high energy milling of elemental powders at ambient temperature which is termed as reaction milling.

The mechano-chemical synthesis (Reaction milling) of metal carbides was proposed by Matteazzi and Caer (1991). They prepared carbides of Ti, V, Cr, Mn, Fe, Co, Ni, Zr, Nb, Mo, Ta, W, Re, Al, and Si by milling the above elements with graphite powder in either a SPEX 8000 shaker mill or a Fritsch P-7 planetary mill for a fixed amount of time. In 1995, El-Eskandarany et al. (1995) prepared stoichiometric SiC powders by solid-state reaction of elemental silicon and carbon powders via the room temperature mechanical alloying process. Complete fcc–SiC alloy powders were obtained after 300 hours of milling. The mechanical alloying process was performed in a high-energy ball mill. Yang and Shaw (1996) also produced SiC from silicon and graphite by attrition milling. Based on the x-ray line broadening they concluded that product compound was β-SiC where the average crystallite size was of the order of 70 nm.

2. REACTION MILLING

Reaction milling is a process where simultaneous milling and chemical reaction takes place in a highly energetic environment. It can be practiced in planetary mills where the force field could be made to vary from one to two orders of magnitude compared to equivalent size ball mills. Reaction milling uses mechanical processing to induce chemical reactions. The major areas where mechano-chemical processing could be applied include ultrafine powder production, mineral and waste processing, metals refining, combustion reactions, production of a fine dispersion of second phase particles, extension of solubility limits, refinement of the matrix microstructure/nanograin formation, formation of amorphous phases. An important feature of mechanochemical process is the refinement of microstructure (i.e., grain size and particle size) associated with simultaneous particle deformation, fracture, and welding processes that accompany ball/powder collision events. The energy transmitted to crystalline powders during

milling may result in dislocation cell structure that develops into random nanostructured grains with increasing milling time. It should be realized that even though nanometer grain sizes are realized during mechano-chemical processing, the particle size typically decreases only to micrometer level.

Planetary milling can induce chemical reactions in a variety of powder mixtures. In fact it has been shown that mechanical activation substantially increases the kinetics of solid-state chemical reactions (Schwarz et al., 1989). In the systems of interest here, reaction does not occur at the beginning of the milling process. However, it becomes possible after a certain activation time, as milling reduces the particle size, thoroughly mixes the components, and increases the number of chemically active defect sites. The activated states or the reaction zones not only increase as particle and grain sizes decrease, but are also regenerated through the repeated particle fracture and welding events. As a consequence, reactions that, due to separation of the reacting phases by the product phases, require high temperatures to occur will occur at low temperatures in a planetary mill without any need for external heating. Thus, a wide range of chemical reactions can be mechanically initiated.

3. PLANETARY MILLING

The dual drive planetary mill consists of a gyratory shaft and two cylindrical steel jars, both are rotated simultaneously and separately at high speed. Such high-speed rotation of both jars and the shaft makes the balls to move strongly and violently, leading to large impact energy of balls that improves the grinding performance. This type of mill has been used not only for grinding but also for mechanical alloying (MA) and mechanochemical (MC) operations (McCormick and Froes, 1998).

The dual drive planetary mill developed specifically for the synthesis of nanocarbides has a rotating shaft that sweeps a circle of diameter 750 mm. The two steel jars of 13.5 cm diameter (2500 ml each) rotate about their own axes around the common axis of the main shaft. The planetary mill is powered by two motors. A 5 HP motor works on the main rotating shaft and a 3 HP motor drives the jars. The rotating speed of both motors can be varied independently and continuously by a frequency controller. Figure 1 shows a configuration of one half of the planetary mill where a jar rotates about a primary axis O. Here *G* is the diameter of rotation of the axis of the jar and *D* is the diameter of the jar itself. Once these parameters are fixed, it turns out, that the planetary mill could be simply characterized by the ratio of the diameter of rotation of the mill axis *G* to the diameter of the mill *D*. Let *R* be the ratio of speed of rotation of the mill axis to the speed of rotation of the mill about its center. Then, if the shaft rotates at an angular velocity of ω, the mill rotates at $R\omega$ on the shaft. A negative value of *R* indicates that the mill and the shaft rotate in opposite direction. During operation, four different kinds of forces act on a ball inside any one of the jars as shown in Fig. 1. These are (i) centrifugal force about the fixed gyrating axes, (ii) centrifugal force about the mill axis, (iii) Coriolis force due to the planetary motion (rotating coordinate system). These forces produce a special acceleration field inside the mill which is difficult to visualize.

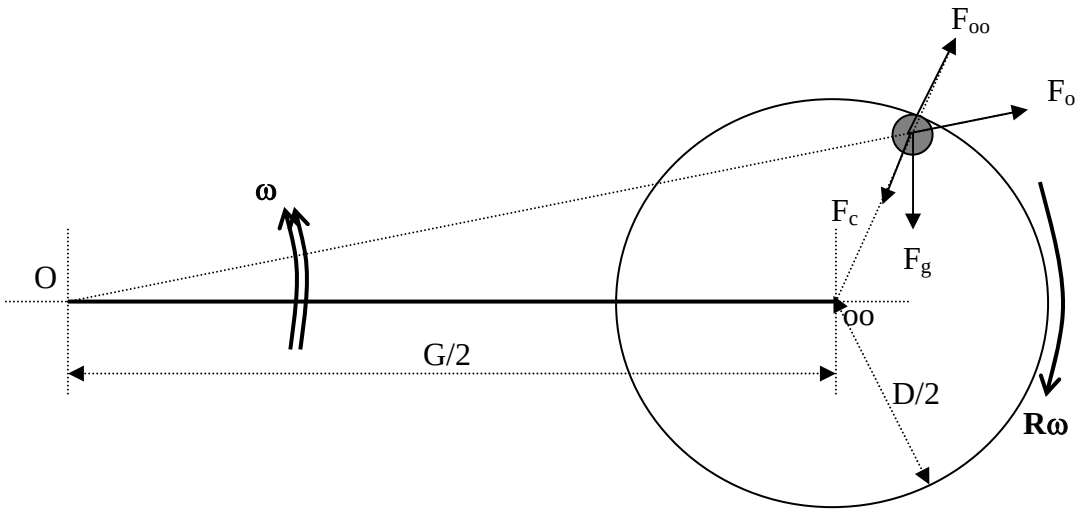

Figure 1. Schematic of the acceleration field in a planetary mill.

The dynamics of the planetary mill dictates that

$$R = -1 \pm \sqrt{\frac{G}{D}}$$

which allows computation of the critical speed. The percent critical speed is

$$\%CS = \frac{N_2}{R \times N_1} \times 100$$

where N_1 is the gyrating speed and N_2 is the jar speed. In our case, the mill was operated at 63% critical speed. This was arrived by doing the following calculation:

$$R = -1 \pm \sqrt{\frac{750}{135}} = -1 \pm 2.36$$

Taking the minus sign for opposite direction of motion between the jar and the main shaft we get,

$$R = -3.36$$

The percent critical speed is calculated by considering the shaft speed and jar speed as 225 and 475 rpm. Therefore

$$\%CS = \frac{475}{3.36 \times 225} \times 100 = 62.8$$

The mechanical description of the milling process is best understood by considering the overall motion of the balls inside the milling chamber and the mechanics of an individual collision including the elastic and plastic deformation of the powder. Much research along these lines was performed in connection with modeling the mechanical alloying process and a summary of these research is available in the literature (Courtney, 1995). It is clear that the force field that exist inside the mill is quite complex and for this reason predicting the motion of the grinding media is not a trivial task. Nonetheless, using the discrete element method (DEM) this complex

motion could be visualized (see Mishra, 1995; Cleary and Hoyer, 2000). DEM not only allows visualization of the dynamic charge mass but also provides information on the frequency of collisions with specific relative velocities that can be used for the modeling purpose.

4. MATERIALS AND METHODS

Starting materials used for milling were silicon and graphite with 99.5 and 99% purity respectively. Steel balls of diameter 6 and 12 mm were used for milling. When setting up a milling experiment, one has to select the number and size of the milling balls and the total mass of the powder. Many investigators choose a ball-to-powder ratio of about 10:1 or a somewhat larger value for a planetary mill. Such conditions work well in most cases. Here, silicon and graphite powders were mixed in 1:1 atomic ratio. Milling was carried out for 40 hours in two jars each containing 125 gm of powder and 2.5 kg steel balls.

Interruption and room temperature aging is known to significantly alter the kinetics of some mechanochemical reactions. However owing practical convenience, all the experiments were carried out for 5 hours on a continuous basis and then the jars were allowed to cool. To prevent agglomeration a dispersant known as 1% by weight of the powder Licowax was added. Once the jar temperature attained the room temperature, it was opened to collect the powder. A small sample was carefully retained for size and X-ray analysis by using the pulversite sample splitter. The remaining powder was put back into the jars and the milling was continued with fresh addition of Licowax. The aging effect at room temperature could not be studied.

The powder samples were analyzed at different intervals of milling time to study the progress of reaction. Powder particles were characterized by X-ray diffraction (CuK_{α}), laser particle size analyzer (Malvern Master sizer 2000), and scanning electron microscope (FEI Quanta).

5. RESULTS AND DISCUSSION

5.1 XRD Analysis

In order to determine the phase change of the particle mixtures during the reaction milling process, a small sample of milled product was repeatedly picked up at regular intervals for X-ray diffraction analysis. Figure 2 shows the XRD graph of powder milled for 40 hours. The two different X-ray patterns correspond to milled powder prepared by using 6 and 12 mm diameter steel balls. In either spectra the peaks corresponding to Si_5C_3, SiC and βSiC are present. However, the intensity of silicon carbide peaks is higher corresponding to the powder that was processed with 12 mm diameter steel balls as compared to the powder processed by 6 mm balls under identical conditions. At the end of the experiment, it was also observed that the 6 mm balls were invariably found coated with the powder whereas no such coating was observed on the 12 mm balls. This shows that the intensity of impact in case of 12 mm diameter ball is sufficient to dislodge any coating that forms on the surface of the ball

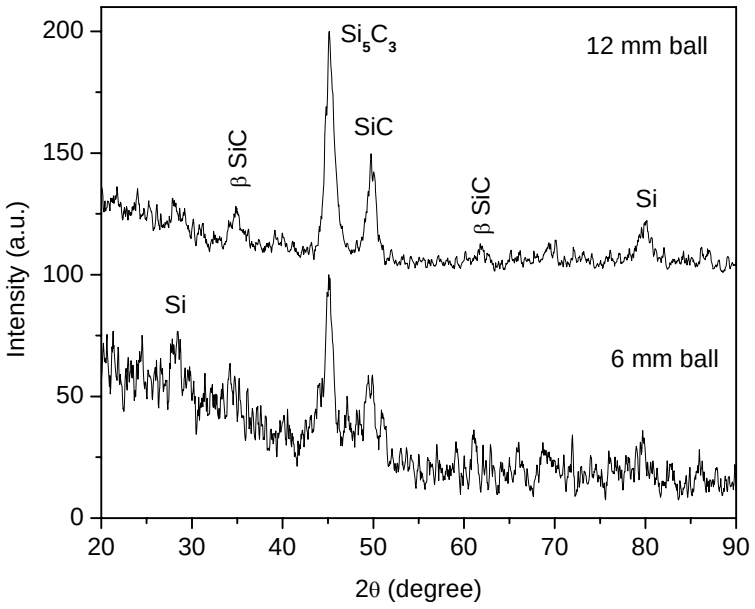

Figure 2. XRD patterns of milled powder at 40 hours of milling times for two different size balls.

The XRD patterns of the end product (as milled SiC powder) is shown in Fig. 3 after different intervals of milling time. Several interesting observations are made. First, the graphite peak

disappeared after about 10 hours of milling. This is a general observation in this study which may be due to amorphization of graphite during milling. However, at this stage the disappearance of the graphite peaks was not accompanied by a shift in the silicon peaks which indicate that there was no formation of Si(C) solid solutions. In fact, the shifts in the peaks suggest that a transitional bonded state between Si and C formed, although no trace of SiC was observed. Second, with increased milling time, silicon peaks also disappeared and silicon carbide peaks were observed. The silicon peak disappeared around 20 hours of milling. Finally, as evident from Fig. 3, the Bragg peaks for the milled product (after about 10 hours of milling) are broad, suggesting the formation of fine grain powders. The crystal size of the as formed SiC was calculated to be between 18 and 10 nm.

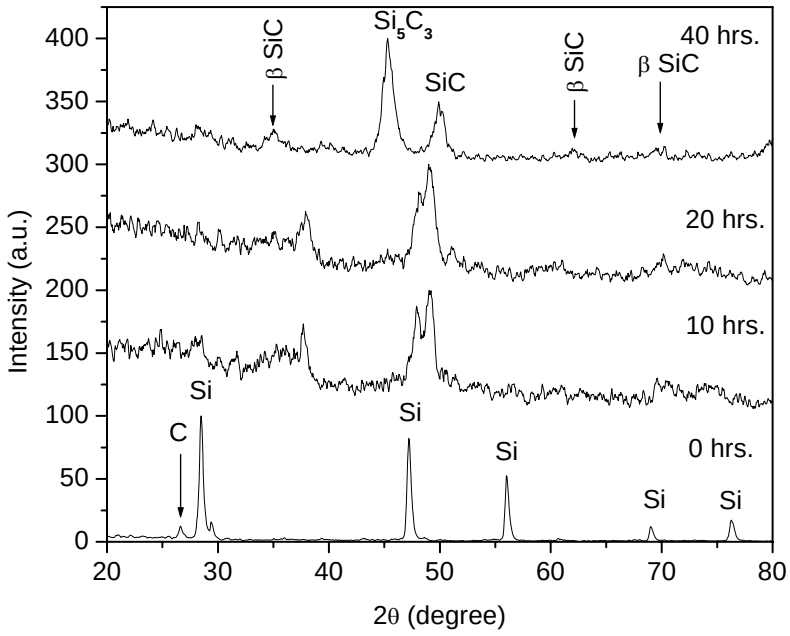

Figure 3. XRD patterns of milled powder at selected milling times.

5.2 Crystal Size and lattice strain

Some features of the activation process can be investigated by X-ray analysis. For this purpose, as received and milled powders were analyzed using X-ray diffraction (XRD) methods

with CuK_α radiation. The XRD peak broadening was used to measure the particle size and internal strain. The broadening due to small crystal size was evaluated through Scherrer formula

$$B_p(2\theta) = \frac{0.9\lambda}{t\cos\theta}$$

where t is the average crystal size, B_p (2θ) is the broadening of the diffraction line measured at full width half maximum intensity (FWHM), λ is the wave length of the x-ray radiation and θ is the Bragg angle. The strain broadening was calculated using

$$B_s(2\theta) = 4\eta\frac{\sin\theta}{\cos\theta}$$

where B_s (2θ) is the broadening due to internal strains and η is the effective internal strains. The total broadening, B_t (2θ), due to both the crystal size and internal strains was assumed to be the linear addition of the two contributions.

$$B_t(2\theta) = \frac{0.9\lambda}{t\cos\theta} + 4\eta\frac{\sin\theta}{\cos\theta}$$

Thus, effects of the crystal size and internal strains on broadening were separated by plotting B_t (2θ) cosθ versus sinθ/λ. Correction for instrumental broadening, which comes due to the superposition of peaks due to $K_{\alpha1}$ and $K_{\alpha2}$, when peaks are not resolved, was taken into account in the measurement of the peak broadening. This was done by running XRD of pre-milled powder under the same conditions as the milled powder. The breadth at half maximum intensity (FWHM) of the desired curve B_t (2θ), which could be obtained if there were no instrumental broadening, was calculated by subtracting breadth of before milled powder from total breadth.

The decrease of the grain size and lattice strain to characterize the activation process has been determined from X-ray diffraction patterns. Although the accumulation of lattice strain is a measure of defect formation, determining the defect structure was found to be more difficult. The crystallite size and the lattice strain of the powder measured from the XRD peak broadening is shown as a function of milling time in Fig. 4. It can be seen that the crystallite size decreases and internal strain increases rapidly with milling time up to about 20 hours. With further milling the crystallite size remains almost constant but internal strain appears to decrease. The decrease in the internal strain after about 20 hours of milling could not be explained. Finally, from Fig. 4 it is noticed that the different mass of the balls results in different crystal size and strain accumulation rates.

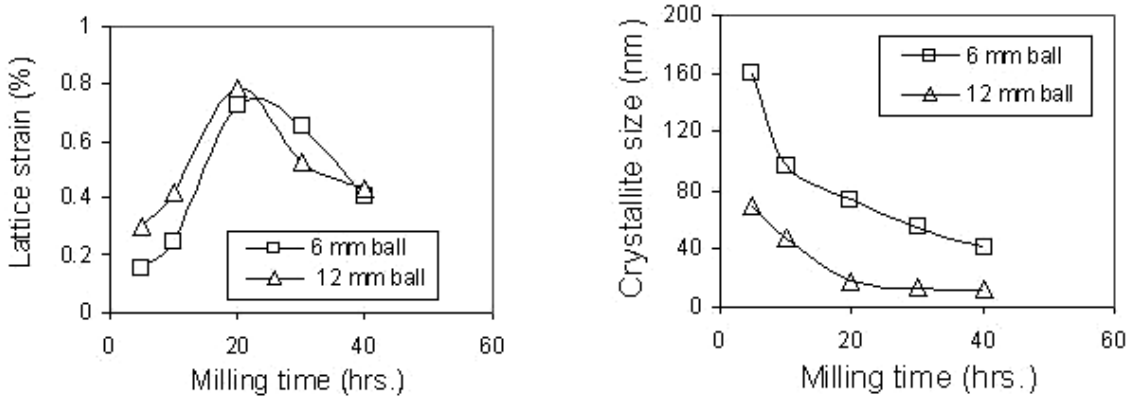

Figure 4. Effect of ball size on lattice strain and the crystallite size of the milled powder calculated from X-ray diffraction patterns; left: lattice strain; right: Crystal size.

5.3 Particle Size

During the early stage of milling, the powder particles of Si and C are mixed together and then mechanically activated such that individual particles of Si and C form composite particles of a larger diameter as a result of cold welding. At a later stage, the solid state reaction starts and considerable amounts of the product (SiC) are formed. Figure 5 shows the particle size distribution of powder at different intervals of milling time. While the d_{25} (25% passing size) size

continuously decreased from 6.5 to 1.45 micron, the d_{75} size initially increased from 25 to 33 micron and then continuously decreased to 17 micron. This type of variation in the size spectra clearly indicates welding of particles at the early stages of milling that could have led to initial increase in particle size. It should be mentioned that the size spectra corresponding to individually milled product of Si and C did not show any evidence of growth in particle size. In TiC system, El-Eskandarany (1996) analyzed the polished and etched particles representing the early stage of grinding. They showed that the individual particle contains many thick layers of the diffusion couples of constituent powders. They believe a solid state reaction takes place at the clean-interfaces of these layers, and a new single phase is formed after further milling. When this happens the reactant layers disappear. Therefore in such systems the only way the particles could grow is by cold welding.

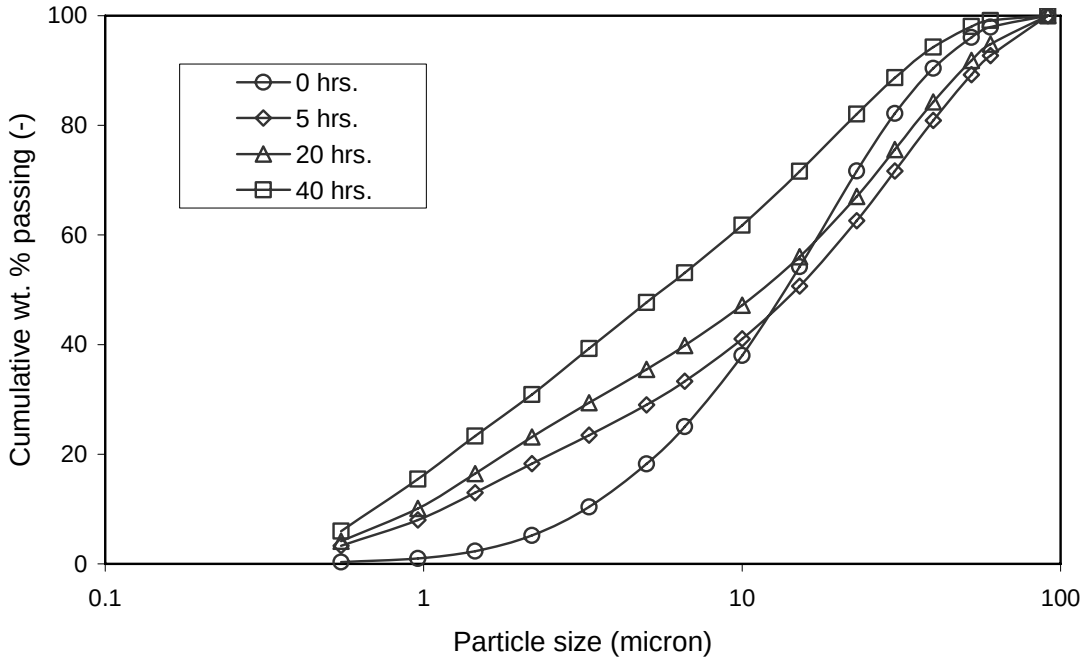

Figure 5. Particle size distribution of the milled product at different intervals of time.

5.4 Temperature

The temperature of outer surface of the jars during milling was measured by a high precision laser pyrometer. The temperature measurements were carried for a total period of 5 hours. During this period milling was carried out continuously. It was observed that after about 3 hours of grinding a steady state condition was attained when the temperature remained constant. The variation in the measured temperature of the outer surface of the jar during milling is shown in Fig. 6. Here the temperature profiles correspond to milling of pure graphite and silicon carbide (Silicon and graphite). It is clear from the figure that the outer surface temperature reach 90 and and 75 ºC during SiC and graphite milling respectively. Under the steady state condition, the temperature of the inner surface of the jar was calculated by a simple heat balance. The measured temperature of the outer surface of the jar and calculated temperature of the inner surface of the jar for different materials are presented in Table 1.

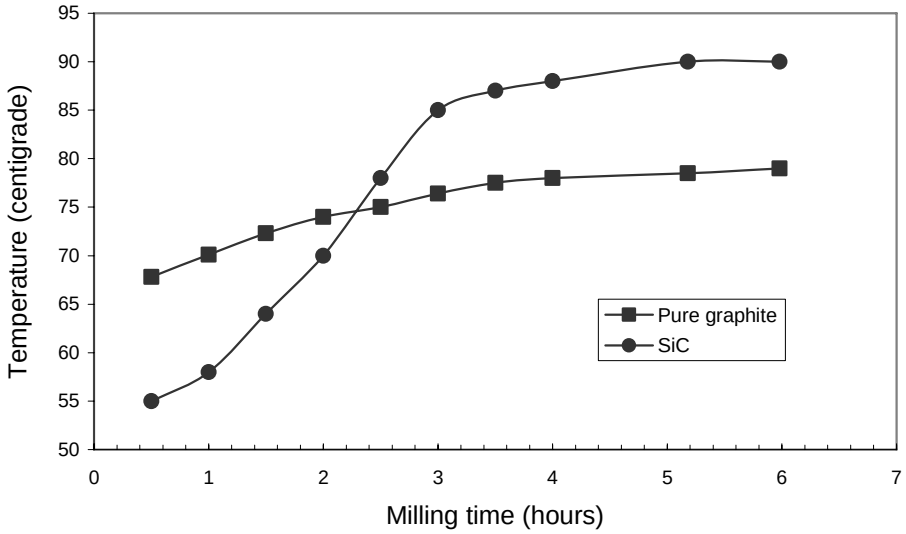

Figure 6. Rise in temperature of the outer surface of the jar.

Table 1. Inside and outside vial surface temperature for different materials.

Materials	Measured outside temperature (°C)	Calculated inside temperature (°C)
Pure iron	116	150

Pure graphite	79	113
Iron + graphite (C: Fe = 1.5)	93	127
Iron + graphite (C: Fe = 2.0)	83	117
SiC	90	124
Limestone	85	119

The actual processing of the powder takes place during the collisions between two balls or a ball and the wall of the mill. From the point of view of reaction milling, a particularly important question is the temperature increase during collision. The possible approaches were reviewed by Koch (1994) and recently worked out in some detail by Murty et al (2004). Depending on the model, rather different estimates of the temperature increase were obtained. For example, when Fe powder was impacted by an 8-mm steel ball, the inner wall temperature was estimated to be 150ºC. These temperatures appear to be sufficient for chemical reaction given the state of mechanical activation achieved in the planetary mill.

5.5 Scanning electron microscopy (SEM)

The SEM technique was used to follow the changes in shape and size of the milled powders during the different stages of the reaction milling process. Figure 7 shows the SEM micrographs of the milled powders after different intervals of milling time. In all the micrographs the marker is set at 50 micron. At the initial stages of milling, the powders of the reactant materials are bulky, with random shape and size. As the milling progressed the powders became spherical as evident from Fig. 7(d) which correspond to 40 hours of milling. As regards particle size. It is also evident from the SEM images that it decreases gradually with increasing milling time. However, concrete evidence of particle coarsening could not be obtained through SEM.

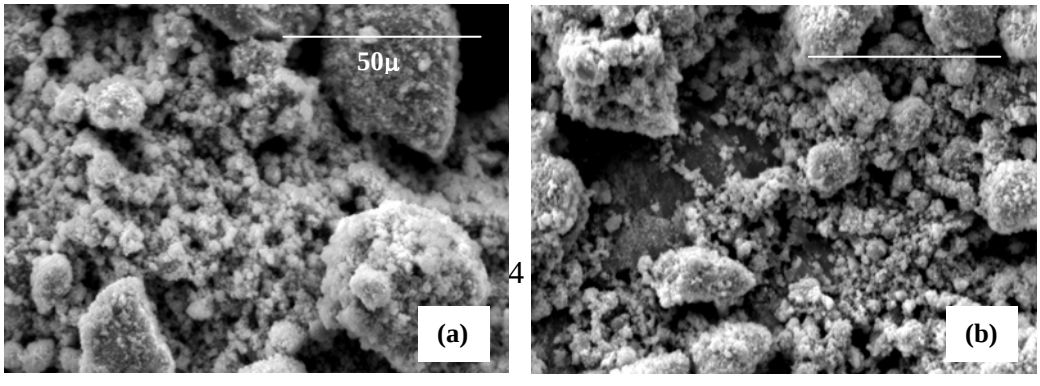

Figure 7. SEM photograph of the powder after (a) 10 (b) 20 (c) 30 (d) 40 hours of milling.

6. CONCLUSIONS

SiC can be synthesized through high-energy reaction milling at room temperature from elemental silicon and graphite powder.

There is an effect of ball size on reaction milling. The amount of impact increases with increasing ball diameter.

As the milling time increases, powder particles become finer and contain more defects. These fine structures developed are prerequisite for the synthesis of crystalline SiC at ambient temperature.

7.0 REFERENCES

1. Vogt, G.J., Vigil, R.S., Newkirk, L.R., and Tukula, M., 1995, Proc. Of the 7th International Symp. On plasma Chemistry, Vol. 2, ed. Timmermans, C.J, Eindhoven, H., International Union of Pure and Applied Chemistry, p. 668.
2. Cannon, W.R., Danforth, S.C., Flint, J.H., Haggerty, J.S., and Marra, R.A., 1982, J. Am. Ceramic Soc. 65, 324.

3. Ritter, J. J., 1995, in Better ceramics through Chemistry II, Materials Research Society Symp. Proc., Vol. 73, eds. Brinker, C.J., Clark, D.E., and Ulrich, D.R, Materials Research Society, Pittsburgh, PA, p. 367.
4. Matteazzi, P., and Caer, G.L., 1991, Journal of Americal Ceramic Society 74 (6), 1382.
5. El-Eskandarany, M.S., Sumiyama, K., Suzuki. K., 1995, Journal of Materials Research 10: 69.
6. Yang, Z.G., and Shaw, L.L., 1996, "Synthesis of nanocrystalline SiC at ambient temperature through high energy reaction milling." Nanostructured Materials, Vol. 7, No. 8, pp. 873-886.
7. Schwarz, R.B., Saw, Petrich, R.R., and Saw, C.K., 1989, Journal of non-crystalline Solids, 76 p. 281.
8. McCormick, P.G., and Froes, F.H., 1998, "The fundamentals of mechanical processing." 1998, Journal of Metals, November 50 (11).
9. Courtney, T. H., 1995, Mater Trans. JIM 36: 110.
10. Mishra, B.K., "Ball charge dynamics in a planetary mill."1995, KONA No. 13, pp. 151-158.
11. Cleary, P. W., Hoyer, D., 2000 "Centrifugal mill charge motion and power draw: comparison of DEM predictions with experiments." International Journal of Mineral Processing 59, pp. 131-148.
12. El-Eskandarany, M. S., 1996, Metall. Trans. A, 27:2374.
13. Koch C.C., 1994, Int. J. Mechanochem Mechanical Alloying 1: 56.
14. Joardar, J., Pabi, S.K., and Murty, B.S. 2004, Scripta Materialia 50 pp. 1199-1202.